A new seven-sample symmetrical phase-shifting algorithm

Kieran G. Larkin * and B.F. Oreb

CSIRO Division of Applied Physics,
PO Box 218, Lindfield, NSW 2070, Australia

* Department of Physical Optics, University of Sydney, NSW 2006, Australia

ABSTRACT

A new seven-sample algorithm has been developed which is particularly useful for phase evaluation in systems with non-sinusoidal periodic waveforms. The algorithm performs well in systems with significant amounts of second, third, fourth and sixth harmonic content and in the presence of phase shift errors. The algorithm is characterised by an equi-spaced symmetrical sampling pattern in which the end samples are one full period apart. Principal features of the algorithm in terms of the Fourier theory of phase-shifting are presented. Performance of the seven-sample algorithm is outlined and compared with several conventional algorithms.

1. INTRODUCTION

There exist a multitude of phase-shifting algorithms which perform well with sinusoidal or near-sinusoidal periodic waveforms[1-5]. However, in applications having non-sinusoidal periodic waveforms (either by choice or through imperfections such as multiple interference or detector non-linearities) the performance of existing algorithms is often inadequate.

Recently a new class of error compensating algorithms has been proposed[6] which combine the harmonic filtering properties of the general N-sample algorithms with the phase-shift error compensating properties of the well known five-sample algorithm[7]. The proposed class of algorithms, termed Symmetrical Phase-Shifting Algorithms (SPSAs) are characterised by the N+1 samples separated by N equal intervals over one full period. Of particular interest in the field of moire profilometry, where the periodic waveform contains significant quantities of second, third and fourth harmonics[8] is the seven-sample symmetrical phase-shifting algorithm. The properties of this algorithm in the presence of harmonics and phase-shifting (often called miscalibration) errors will be presented. The full derivation of the general N+1 sample SPSA is lengthy and will not be presented here. However, the important properties of phase-shifting algorithms as described in the Fourier domain will be illustrated with two examples: the five-sample algorithm[7] and the seven-sample SPSA.

2. ERROR COMPENSATING SCHEMES

The performance of phase-shifting algorithms in the presence of various errors has been the subject of numerous publications [1,3,7,9-15]. Often the analysis has been performed on an algorithm by algorithm basis. Until recently the mechanism of error propagation has been seen as essentially different for each algorithm and not easily generalized[16]. This has given rise to many schemes and algorithms for

0-8194-0928-6/93/$4.00

compensating specific types of errors. Perhaps the best known algorithm which compensates consistent phase-shift errors is that of Carre[5]. Also well known is the five-sample algorithm [7,9] which compensates for phase-shift errors to the first order only. In addition to these there are several so-called "averaging" techniques which involve two phase calculations with a 90° increment between them[9]. In many cases the error compensating algorithm has arisen as a solution to a specific measurement problem. The phase-shifting technique has been generalised to N-sample algorithms using the method of least squares [17,18]. Subsequently the general harmonic properties of the N-sample algorithm were identified[3]. Unfortunately this harmonic analysis has been frequently misinterpreted primarily because of the unclear distinction between harmonic errors in the numerator/denominator of the arctangent function and harmonics in the phase error[16]. The situation has clarified with a comprehensive Fourier description of the phase-shifting process[19]. The introduction of filter functions[19], which remove certain frequency components of the signal, provides a way of visualizing the performance parameters of various algorithms. In particular it can be readily shown that the general N-sample algorithm is insensitive to errors caused by all harmonics up to (N-2) in the signal. For example, the common four-sample (90°) algorithm is unaffected by second harmonic components in the signal.

A common feature of error compensating algorithms is the presence of an additional sample in the sense that it is not required by the least squares method. This extra sample effectively conveys information about the phase-shift increment. The compensating algorithm automatically adapts to incorrect phase-shift whereas a conventional algorithm relies on the phase-shift being correct.

In the following sections we will adopt the convention of referring to any algorithm derived from the least square analysis [17,18] as an "N-sample algorithm". In contrast to this an algorithm belonging to the class of SPSA's will be called an "N+1 SPSA". For example, the well known five-sample algorithm [7] shall now be referred to as the 4+1 SPSA. Also the seven-sample algorithm of this paper's title shall be referred to as the 6+1 SPSA. It is important to note that the N+1 SPSA and the N-sample algorithm have the same phase-shift between samples.

3. FOURIER DESCRIPTION OF PHASE-SHIFTING ALGORITHMS

Fourier techniques have been applied extensively to the area of interferogram analysis[20]. A whole branch of analysis based on the Fourier transform method applied to fringe patterns has been developed[21]. The Fourier technique developed by Freischlad[19] is used to characterise the phase-shift algorithms which are applied to fringe pattern analysis. More recently a very similar Fourier technique has been developed (independently it seems) for moire pattern analysis[22]. The full Fourier description of the phase-shifting process has been presented in two papers [6,19]. The main points of interest arising from these papers will now be summarised to enable the principal properties of SPSAs to be illustrated graphically.

Virtually all phase-shifting algorithms involve the calculation of an arctangent function. The argument of the arctangent is composed of a numerator and denominator. It can be shown[19] that the numerator and the denominator can be represented as correlations of the signal with sampling functions. The calculation of phase can be written as:

$$\Phi = \tan^{-1} \frac{c_1(0)}{c_2(0)} \qquad (1)$$

where Φ is a function of x and y as are c_1 and c_2 but the explicit variation has been omitted because it is assumed that the calculation is performed on just one point (which may be any point). $c_1(t)$ and $c_2(t)$ are correlations expressed as functions of the generalized shift parameter t. Consider a signal (interferogram or a fringe pattern) g(x,y,t) where g is a periodic function of t, but not necessarily of x and y. Figure 1 shows a periodic function g, with period T_g plotted against the shift parameter t. Figure 1 also shows the modulus of the Fourier transform of g defined by $|G(\nu)|$, where

$$G(\nu) = \int_{-\infty}^{\infty} g(t)\, e^{-2\pi i \nu t}\, dt \; . \qquad (2)$$

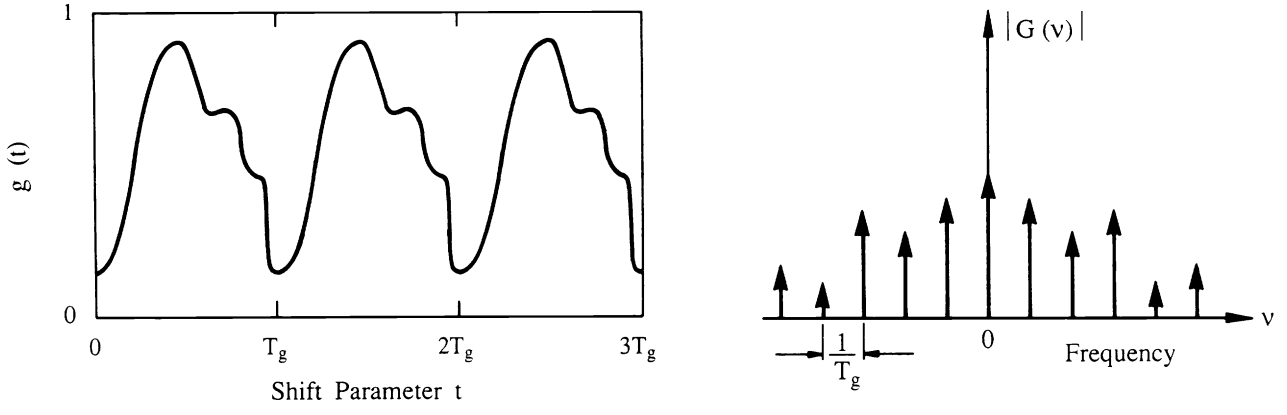

Figure 1. Periodic function g(t) and the modulus of its transform G(ν).

It is important to note that this is a one-dimensional Fourier transform relative to the t parameter and not relative to the spatial variables x and y. As the signal g(t) is periodic, the transform $G(\nu)$ is discrete - only certain frequencies are present. The correlations mentioned above can be written as

$$c_1(t) = \int_{-\infty}^{\infty} g(\tau)\; f_1(t+\tau)\, d\tau \qquad (3)$$

and similarly for $c_2(t)$ and $f_2(t)$. The functions $f_1(t)$ and $f_2(t)$ are sampling functions (Freischlad[19] calls them filter functions). Figure 2 shows the sampling functions f_1 and f_2 for the well known 4+1 SPSA[7]. The arrows represent delta (δ) functions which symbolize the sampling process. The length of each arrow represents the weight associated with that sample. Zero weighted samples are shown as large dots (•). The sine and cosine envelopes are shown by the dotted lines. The full sampling period or total shift is T_f (usually $T_f = T_g$). Figure 3 shows the Fourier transforms of $f_1(t)$ and $f_2(t)$ which are $F_1(\nu)$ and $F_2(\nu)$ respectively. A key result of the Fourier description is

$$c_1(0) = 2\mathrm{Re}\left\{ \int_0^{\infty} G(\nu)\; F_1^{*}(\nu)\, d\nu \right\} \qquad (4)$$

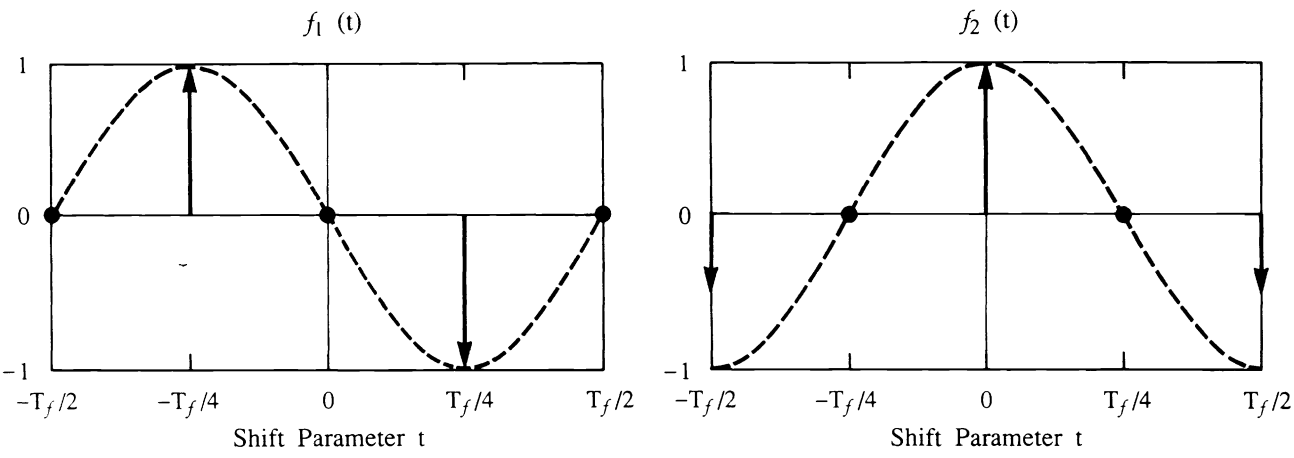

Figure 2. Sampling functions $f_1(t)$ and $f_2(t)$ for the five (4+1) sample algorithm.

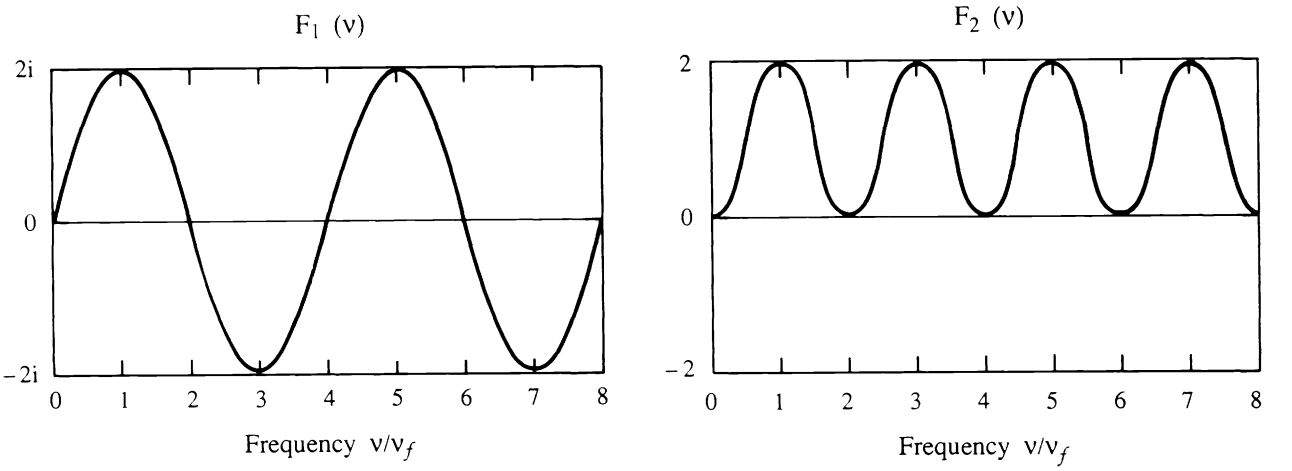

Figure 3. Sampling function spectra $F_1(\nu)$ and $F_2(\nu)$ for the five (4+1) sample algorithm.

where Re stands for the real part and * indicates complex conjugation. This equation determines how the signal spectrum $G(\nu)$ is modified by the sampling function spectrum $F_1(\nu)$. A similar relation holds for $c_2(0)$ and $F_2(\nu)$. The analysis is further simplified because $G(\nu)$ is a discrete function, therefore

$$c_1(0) = g_0 F_1(0) + 2\mathrm{Re}\left\{ \sum_{n=1}^{\infty} g_n F_1^{*}(n\nu_g) \right\} \qquad (5)$$

where $\nu_g = {}^{1}/T_g$

and

$$G(\nu) = \sum_{n=-\infty}^{\infty} g_n \, \delta(\nu - n\nu_g) \; . \qquad (6)$$

In other words the numerator of the arctangent, $c_1(0)$, is formed from components g_n of the discrete signal spectrum multiplied by the corresponding sampling function spectrum $F_1^*(n\nu_g)$. The components are summed and the real part is extracted. The denominator is formed similarly. The performance of any phase-shift algorithm can thus be simply analysed. First, from a knowledge of the phase increments and the sample weights the filter functions $F_1(\nu)$ and $F_2(\nu)$ are formed. Then the signal spectrum $G(\nu)$ is multiplied by these filter functions and a summation of frequency components performed. The real parts of the two summations form the numerator and the denominator of the arctangent function, $c_1(0)$ and $c_2(0)$ respectively. A recent analysis[16] of the arctangent function shows how all harmonic components of both numerator and denominator are frequency-shifted when the arctangent is evaluated. Particular attention should be paid to the location of zeroes in both $F_1(\nu)$ and $F_2(\nu)$. In figure 3 the zeroes occur at all even harmonics, a result consistent with past observations of the insensitivity of the 4+1 SPSA to second harmonic signal components. Also shown clearly in figure 3 are the maxima occurring at the fundamental sampling frequency (n=1) in both F_1 and F_2. The rates of change of both these function are equal to zero at the fundamental. Thus in systems with a small detuning of the sampling frequency will have approximately the same values of $F_1(\nu)$ and $F_2(\nu)$ as a system without detuning. This is closely related to an algorithm's property of eliminating phase errors due to incorrect phase-shift increments. A detailed error analysis[6] has revealed that this type of phase error will be corrected in an algorithm which has equal relative gradients of the sampling functions spectra at the fundamental frequency. This may be written as follows:

$$\frac{1}{F_1} \cdot \frac{dF_1(\nu)}{d\nu} = \frac{1}{F_2} \cdot \frac{dF_2(\nu)}{d\nu} \qquad (7)$$

at $\nu = \nu_f$ where $\nu_f = {}^1/T_f$

The above condition is satisfied for all SPSAs. In essence it means that the relative gradients of both F_1 and F_2 must be matched if error compensation is to occur.

The derivation of the generalized N+1 SPSA has been carried out in the Fourier domain[6]. It is also possible to derive in the real (i.e. the shift parameter t) domain. The Fourier derivation really begins to show advantages in situations where the input signal contains harmonics. At this stage the real domain analysis becomes unwieldy and is, perhaps at best, only suitable for computer simulation.

4. THE 6+1 SYMMETRICAL PHASE-SHIFTING ALGORITHM

The 6+1 SPSA has arisen as a solution to the measurement problems inherent in a projected fringe profilometer system[8]. Early work using the 4+1 SPSA demonstrated the need for algorithms with even lower systematic error levels.

The 6+1 SPSA is written as follows,

$$\tan \Phi = \frac{\sqrt{3}\,(I_2 + I_3 - I_5 - I_6) + (I_7 - I_1)/\sqrt{3}}{(-I_1 - I_2 + I_3 + 2I_4 + I_5 - I_6 - I_7)} \qquad (8)$$

I_1 through to I_7 represent samples with 60° phase shifts between each sample.

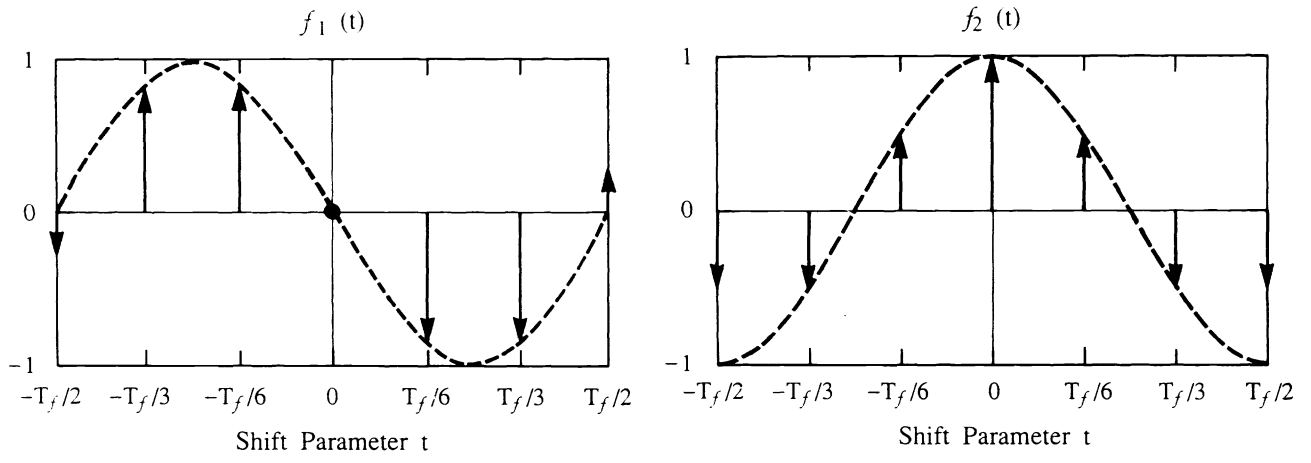

Figure 4. Sampling functions $f_1(t)$ and $f_2(t)$ for the seven (6+1) sample algorithm.

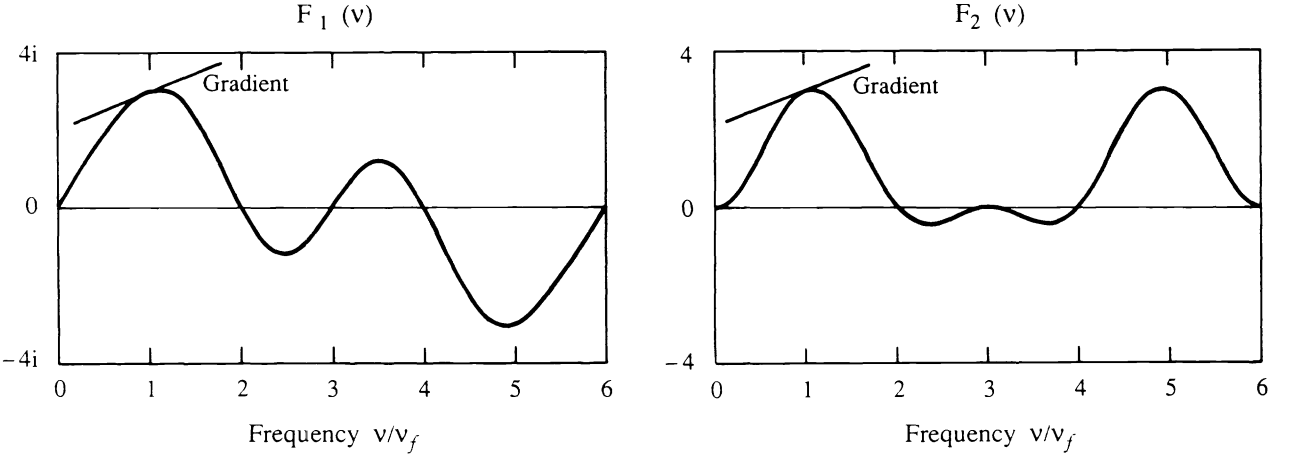

Figure 5. Sampling function spectra $F_1(v)$ and $F_2(v)$ for the seven (6+1) sample algorithm. Note the gradients at $v = v_f$.

Figure 4 shows the corresponding numerator and denominator sampling functions $f_1(t)$ and $f_2(t)$ for the 6+1 SPSA. The denominator function can be derived from a weighted least-squares fit to a cosine. The derivation of the numerator is more involved, but is based on a least squares sine fit with the addition of end samples (here I_1 and I_7).

With reference to $f_1(t)$ in Figure 4, the end samples occur where the sinusoidal envelope has zero amplitude. Normally, in a system with correct phase-shifting (i.e. a perfectly calibrated phase-shifting mechanism) the end samples I_1 and I_7 are equal and so $I_7-I_1 = 0$ and these samples do not contribute to the numerator. In a situation with some miscalibration of the phase shifter an error occurs in the denominator. This error is exactly cancelled by a corresponding error in the numerator. The (I_7-I_1) term ensures exact cancellation.

In the Fourier domain a parallel argument can be stated. Figure 5 shows the sampling function spectra $F_1(\nu)$ and $F_2(\nu)$ for the 6+1 algorithm. Consider a system with correct phase-shifting and a sinusoidal input signal g(t). The numerator of the arctangent will contain one harmonic component determined by $F_1(\nu_f)$ where $\nu_f = \nu_g$, the signal frequency. Similarly the denominator will contain a component determined by $F_2(\nu_f)$. In this case it can be shown that[6] $F_1(\nu_f) = i\ F_2(\nu_f)$ where the i factor indicates that the components are in quadrature. If, however, there is some miscalibration then the fundamental sampling frequency ν_f is no longer equal to the signal frequency ν_g and so the harmonic components must be evaluated at multiples of $(\nu_f + \Delta\nu)$ where $\Delta\nu$ represents the frequency increment due to miscalibration. For the phase error to be corrected in this case the following relation must be satisfied:

$$F_1(\nu_f + \Delta\nu) = i\ F_2(\nu_f + \Delta\nu) \qquad (9)$$

The above equation can be written as a Taylor series expansion. If only first order terms are considered then the matched gradients expression for F_1 and F_2 in equation (7) results.

Referring again to Figure 5 we can see that the gradients of both F_1 and F_2 at the fundamental frequency are matched, in other words equation (7) is satisfied. This explains the insensitivity of the 6+1 SPSA to miscalibration errors.

5. PERFORMANCE OF THE 6+1 SPSA

To get a feeling for the utility of this new phase-shifting algorithm we have evaluated phase errors for five algorithms implemented by the phase-stepping rather than integrating-bucket technique. Two error sources are considered simultaneously. The first source is the harmonic content in the input signal. The input signal used has the following components which are not unusual in projected fringe systems:

fundamental	taken as 100%
second harmonic	30%
third harmonic	6%

The second source of error is the miscalibration of phase-step. The error is expressed as a percentage (p) of the ideal step size. For example, instead of moving 100% of 90° phase-shift required the system actually moves (100+p)% of 90° (or 60° for the six-sample and the 6+1 SPSA). Table 1 contains a summary of the phase calculation errors related to the five algorithms, namely the four-sample (90°), the 4+1 SPSA, the six-sample (60°), the seven-sample (51.4°) and the 6+1 SPSA. The resulting phase errors are tabulated as four harmonics. Note that the figures shown are percentage phase errors where 100% corresponds to 180° (π radians). So, for a 10% (p=10) phase-step error the four-sample algorithm will produce a second harmonic phase error of 2.05% (equivalently 3.69°).

Some aspects of Table 1 deserve comment. The values in the table are derived from the small angle approximation outlined elsewhere [15,16]. Both the four-sample and the 4+1 sample algorithms give a fixed quantity of fourth harmonic error, almost 2%. This is unacceptably large in a high precision phase-shifting system. Note,

however, that the 4+1 SPSA eliminates second harmonic errors. Comparing the six-sample and the 6+1 sample algorithms we find that the 6+1 SPSA has very low second, third and fourth harmonics but the first harmonic error is higher. Comparing the conventional seven-sample algorithm with the new 6+1 SPSA, the second harmonic is clearly much smaller in the new algorithm. Third and fourth harmonics for both algorithms are small. Again it is only the first harmonic of the new algorithm which is somewhat larger.

TABLE 1. Errors in calculated phase (expressed as a percentage of 180°) for several phase-shifting algorithms

		PHASE-SHIFTING ALGORITHM				
		FOUR SAMPLE (90°)	FIVE (4+1) SAMPLE SPSA	SIX SAMPLE (60°)	SEVEN SAMPLE (51.4°)	SEVEN (6+1) SAMPLE SPSA
HARMONIC	1	0.260 p	0.150 p	0.173 p	0.179 p	0.231 p
	2	0.205 p	0	0.163 p	0.227 p	0.017 p
	3	0.212 p	0.150 p	0.200 p	0.058 p	0.058 p
	4	1.910	1.910	0.031 p	0.012 p	0.017 p

Note that p is the percentage phase-shifting error (miscalibration).

6. CONCLUSION

The most suitable algorithm for a particular measurement configuration will depend on the source errors. The error compensating properties of the new algorithm are related to certain properties of sampling functions expressed in the Fourier domain. The gradients and zero crossings of the functions $F_1(\nu)$ and $F_2(\nu)$ determine algorithm performance and are easily represented graphically. The new seven (6+1) sample algorithm has been shown to have excellent performance with respect to second, third and fourth harmonic in calculated phase.

7. REFERENCES

1. K. Creath, "Phase-Measurement Interferometry Techniques", *Progress in Optics XXVI*, edited by E. Wolf, 349-393, Elsevier Science Publishers, Amsterdam, 1988.

2. J.C. Wyant, "Interferometric Optical Metrology: Basic Principles and New Systems", *Laser Focus*, 65-71, May 1982.

3. K.A. Stetson and W.R. Brohinsky, "Electro Optic Holography and its Application to Hologram Interferometry", *App. Opt.* 24, (21), 3631-3637, 1985.

4. P. Hariharan, B.F. Oreb and N. Brown, "Real time holographic interferometry: a microcomputer system for the measurement of vector displacements", *App. Opt.* **22**, 876-880, 1983.

5. P. Carre, "Installation et Utilisation due Comparator Photoelectrique et Interferential du Bureau International des Poids et Mesures", *Metrologia*, **2**, (1), 13-23, 1966.

6. K.G. Larkin and B.F. Oreb, "Design and Assessment of Symmetrical Phase-Shifting Algorithms", To appear in *J. Opt. Soc. Am. A.*

7. P. Hariharan, B.F. Oreb and T. Eiju, "Digital Phase-Shifting Interferometry: a simple error-compensating phase calculation algorithm", *App. Opt.* **26**, 2504-2506, 1987.

8. B.F. Oreb, K.G. Larkin, P.S. Fairman and M. Ghaffari "Moire Based Optical Surface Profiler for the Minting Industry", *SPIE Proceedings Vol.* 1776, SPIE Conf. on Interferometry: Surface Characterization and Testing, San Diego, July 1992.

9. J. Schwider, R. Burow, K.-E. Elssner, J. Grzanna, R. Spolaczyk and K. Merkel, "Digital Wave-Front Measuring Interferometry: Some Systematic Error Sources", *App. Opt.* **22**, 3421-3432, 1983.

10. K. Kinnstaetter, A. Lohmann, J. Schwider and N. Streibl, "Accuracy of Phase Shifting Interferometry", *App. Opt.* **27**, 5082-5089, 1988.

11. J. Schwider, "Phase Shifting Interferometry: Reference Error Reduction", *App. Opt.* **28**, (18), 3889-3892, 1989.

12. P. Hariharan, "Digital Phase-Stepping Interferometry: Effects of Multiply Reflected Beams", *App. Opt.* **26**, 2506-2507, 1987.

13. C. Ai and J.C. Wyant, "Effect of piezoelectric transducer nonlinearity on phase-shift interferometry", *App. Opt.* 26, (14), 1112-1116, 1987.

14. J. Schwider, "Advanced Evaluation Techniques in Interferometry", *Progress in Optics XXVIII*, edited by E. Wolf, Chapter IV, Elsevier Science Publishers, Amsterdam, 1990.

15. J. van Wingerden, H. J. Frankena and C. Smorenburg, "Linear Approximation for Measurement Errors in Phase Shifting Interferometry", *App. Opt.* **30**, (19), 2718-2729, 1991.

16. K.G. Larkin, B.F. Oreb, "Propagation of errors in different phase-shifting algorithms: a special property of the arctangent function", *SPIE Proceedings Vol. 1755*, SPIE Conf. on Interferometry: Techniques and Analysis, San Diego, July 1992.

17. C.J. Morgan, "Least Squares Estimation in Phase-Measurement Interferometry", *Opt. Lett.* 7, 368-370, 1982.

18. J.E. Grievenkamp, "Generalised Data Reduction for Heterodyne Interferometry", *Opt. Eng.* **23**, 350-352, 1984.

19. K. Freischlad and C.L. Koliopoulos, "Fourier Description of Digital Phase-Measuring Interferometry", *J. Opt. Soc. Am. A.* **7**, (4), 542-551, 1990.

20. K.H. Womack, "Frequency domain description of interferogram analysis", *Opt. Eng.* 23, 396-400, 1984.

21. M. Takeda and K. Mutom, "Fourier transform profilometry for the automatic measurement of 3-D object shapes", *App. Opt.* **22**, (24), 3977-3982, 1983.

22. D.H. Parker, "Moire patterns in three-dimensional Fourier space", *Opt. Eng.* 30, 1534-1541, 1991.